IRAS 01202+6133 : A Possible Case of Protostellar Collapse Triggered by a Small HII Region

Sung-Ju Kang and C. R. Kerton

Department of Physics & Astronomy, Iowa State University, Ames, IA 50011, USA

sjkang@iastate.edu, kerton@iastate.edu

ABSTRACT

We present an analysis of HCO^+ ($J = 3 \rightarrow 2$) and $H^{13}CO^+$ ($J = 3 \rightarrow 2$) observations of the massive (M$\sim$ 20 $M_\odot$) submm/IR source IRAS 01202+6133 located on the periphery of the H II region KR 120 (Sh 2-187). The HCO^+ line profile has a classic blue-asymmetric shape with the optically thin $H^{13}CO^+$ line peaking at the position expected if the HCO^+ line arises from a combination of self-absorption and infall motion. We have modified existing analytic radiative transfer models to allow for the fitting of submm/mm line profiles that have both self-absorption features and optically thin wings and applied these models to our HCO^+ spectrum of IRAS 01202+6133. We conclude that it is a young Class I YSO with a substantial envelope undergoing slow infall and having some outflow motions. The young age of the H II region rules out a "collect and collapse" scenario. While we cannot eliminate the possibility that IRAS 01202+6133 formed spontaneously at its current location, considering its early evolutionary state and its proximity to the H II region we think that the formation of IRAS 01202+6133 was triggered by the expansion of KR 120 (Sh 2-187).

Subject headings: ISM: molecules – ISM: kinematics and dynamics – H II regions – stars: formation – Line: profiles

1. Introduction

The molecular gas surrounding an H II region is thought to be a place where star formation can be induced. Such triggered star formation can arise from the overpressurization of existing density enhancements (Thompson et al. 2004) or through the collapse of a swept up layers of material (Elmegreen 1998; Deharveng et al. 2003). This paper presents an analysis of submm spectroscopic observations of the Class I Young Stellar Object (YSO) IRAS 01202+6133 which is located on the periphery of the relatively

nearby ($d = 1.44 \pm 0.26$ kpc) H II region KR 120 (Sh 2-187; Arvidsson & Kerton 2011; Kalas & Reich 1980; Sharpless 1959). As shown in Figure 1 the proximity alone of this massive ($M = 21 \pm 9$ $M_\odot$), luminous ($L \sim 5600$ $L_\odot$) YSO to the H II region makes it a strong candidate for an example of triggered star formation. The submm spectra presented here strengthen this scenario as they clearly show infall is occurring as would be expected for a very young YSO. We believe that IRAS 01202+6133 is one of the clearest examples to date of an H II region triggering the formation of another massive star.

Our observations are described in § 2. In § 3 we review the analytic models of Myers et al. (1996) and DeVries & Myers (2005) and develop new varieties of these models that allow for both infall and outflow motions. Physical properties of the YSO derived using these models are presented and discussed in § 4 followed by our conclusions in § 5.

2. Observations

In order to explore the kinematics of IRAS 01202+6133 we obtained observations of the commonly used (e.g., Sun & Gao 2009) optically thick infall tracer molecule HCO^+ ($J = 3 \rightarrow 2$; 267.6 GHz) and its optically thin isotopologue $H^{13}CO^+$ ($J = 3 \rightarrow 2$; 260.3 GHz) at the James Clerk Maxwell Telescope (JCMT) in the 06B semester. Single pointing observations (beamsize $\sim 20''$ FWHM) were made using the A3 receiver and ACSIS backend with a frequency resolution of 61 kHz (0.068 km s^{-1}) and an integration time of ~ 40 minutes for each line. The reduced spectra are shown in Figure 2. Both have a noise level of ~ 0.1 K resulting in a peak S/N$\sim$ 30 for the HCO^+ spectrum and $\sim$ 3 for the weaker $H^{13}CO^+$ spectrum.

If there was no infall motion associated with IRAS 01202+6133 we would expect the HCO^+ spectrum to be a single self-absorbed profile with symmetric red and blue peaks around a local minimum at some systematic velocity. Following Myers et al. (1996), in the case of where there is infall there will be density and excitation temperature (T_{ex}) differences between the central regions and the outer parts of the molecular core. Blueshifted emission from the rear of the core is not strongly absorbed because it passes through the central (high T_{ex}) region then through a highly Doppler shifted front portion of the core. In contrast the redshifted emission from the front of the core is absorbed by surrounding gas that is at both a comparable velocity and similar (low) T_{ex}. The overall effect of the infall motion is to create a "blue-asymmetric" line profile where the self-absorption line is asymmetric with a stronger blue peak. Such a line profile could also form from multiple unrelated emission components being aligned along the line of sight or from rotational motion, but in both cases we would expect to see a similar profile in the optically thin line. The fact that our $H^{13}CO^+$ spectrum

peaks up at the same velocity as the minimum in the HCO^+ spectrum makes us confident that we are looking at a single self-absorbed line profile with the asymmetry arising from infall motions.

3. Analytic Radiative Transfer Modeling

Myers et al. (1996) and DeVries & Myers (2005) developed basic one-dimensional (1D) analytic radiative transfer models to derive kinematic data from mm/submm spectra of star-forming molecular cores. In this section we first review these models and then present modified versions that better model cases where there is simultaneous infall and outflow motions.

All of the models are based on the general solution to the 1D radiative transfer equation for a homogeneous medium with total optical depth τ_0,

$$T_B = T_i e^{-\tau_0} + \int_0^{\tau_0} J(T) e^{-\tau} d\tau \tag{1}$$

where T_B is the brightness temperature of the outgoing radiation, T_i is the brightness temperature of any incoming radiation, $J(T) \equiv T_0/[\exp(T_0/T) - 1]$ and $T_0 \equiv h\nu/k$, where ν is the frequency of the transition and T is the temperature.

If $J(T)$ is a linear function of τ then equation 1 can be integrated to obtain,

$$T_B = T_i e^{-\tau_0} + (J_2 - J_1)\frac{1 - e^{-\tau_0}}{\tau_0} + J_1 - J_2 e^{-\tau_0} \tag{2}$$

where J_1 and J_2 are the values of $J(T)$ at the two ends of the path with optical depth τ_0. All of the models presented in this section are based on equation 2 with variations due to how $J(T)$ varies with τ in detail.

3.1. Two-layer model

The two-layer model of Myers et al. (1996) has "front" and "rear" constant T_{ex} layers moving toward each other each at an infall velocity, v_{in} (see Figure 1 of DeVries & Myers 2005).

The line brightness temperature of the two-layer model is

$$\Delta T_B = J(T_f)[1 - e^{-\tau_f}] + J(T_r)[1 - e^{-\tau_r}]e^{-\tau_f} - J(T_b)[1 - e^{-\tau_f - \tau_r}] \tag{3}$$

where T_f and T_r are the front and rear excitation temperatures and T_b is the background temperature. The optical depths of each layer, τ_f and τ_r are given by

$$\tau_f = \tau_0 \exp\left[-(v - v_{LSR} - v_{in})^2/2\sigma^2\right], \quad (4a)$$

$$\tau_r = \tau_0 \exp\left[-(v - v_{LSR} + v_{in})^2/2\sigma^2\right] \quad (4b)$$

where τ_0 is the line center optical depth, v_{LSR} is a average line-of-sight velocity of the system, and σ is the velocity dispersion of the observed molecule.

For a given choice of T_b (usually $T_b = 2.7$ K) the two-layer model has six adjustable parameters: T_f, T_r, τ_0, v_{LSR}, v_{in}, and σ. By making some assumptions about the expected density and temperature structure in an infalling core Myers et al. (1996) was able to reduce the number of parameters in the two-layer model to five, replacing T_r and T_f by a kinetic temperature, T_k. This version of the model also used the non-thermal velocity dispersion as an input, $\sigma_{NT} \equiv (\sigma^2 - kT_k/m_{obs})^{1/2}$ where m_{obs} is the mass of the observed molecule. Here we present the formulas used to calculate the model parameters and refer the reader to Myers et al. (1996) for their derivation.

The excitation temperature of each layer is determined using the following equations,

$$\frac{T_f}{T_k} = \frac{T_b + (4T_0/\beta)\langle n_f\rangle/n_{max}}{T_k + (4T_0/\beta)\langle n_f\rangle/n_{max}}, \quad (5a)$$

$$\frac{T_r}{T_k} = \frac{T_b + (4T_0/\beta)\langle n_r\rangle/n_{max}}{T_k + (4T_0/\beta)\langle n_r\rangle/n_{max}}, \quad (5b)$$

where $\beta = [1 - \exp(-\tau_0)]/\tau_0$, and $\langle n_f\rangle/n_{max}$ and $\langle n_r\rangle/n_{max}$ are given by,

$$\frac{\langle n_f\rangle}{n_{max}} = (1 - e^{-\tau_0})^{-1}\left[\frac{6}{\tau_0^3} - e^{-\tau_0}(1 + \frac{3}{\tau_0} + \frac{6}{\tau_0^2} + \frac{6}{\tau_0^3})\right], \quad (6a)$$

$$\frac{\langle n_r\rangle}{n_{max}} = (1 - e^{-\tau_0})^{-1}[1 - \frac{3}{\tau_0} + \frac{6}{\tau_0^2} - \frac{6}{\tau_0^3}(1 - e^{-\tau_0})]. \quad (6b)$$

3.2. Hill model

In the "hill" model of DeVries & Myers (2005) $J(T)$ increases linearly from the T_0 to T_p over a front optical depth (τ_f), and then decreases from T_p to T_0 over a rear optical depth (τ_r). The shape of a $J(T)$ plot against τ gives the model its name (see Figure 1 of DeVries & Myers 2005). As with the two-layer model the front and rear sections each have a

line center optical depth (τ_0), are moving toward each other with an infall velocity v_{in}, and have a velocity dispersion σ.

The line brightness temperature of the hill model[1] is given by,

$$\Delta T_B = [J(T_p) - J(T_0)] \left[\frac{1 - e^{-\tau_f}}{\tau_f} - \frac{e^{-\tau_f}(1 - e^{-\tau_r})}{\tau_r} \right] + [J(T_0) - J(T_b)] \left(1 - e^{-\tau_f - \tau_r}\right). \quad (7)$$

For a given choice of T_b, the hill model has six adjustable parameters: T_0, T_p, τ_0, v_{LSR}, v_{in}, and σ. Equations 4a and 4b are used to determine τ_f and τ_r.

3.3. Analytical models with outflow

While the two-layer and the hill models are able to reproduce the central portion of the observed blue-asymmetric line profile they are not able to model the extended wings of the line profile observed beyond $\sim \pm 2$ km s^{-1} (see Figure 3). In order to correctly model the entire line we follow the approach used in the Myers et al. (1996) analysis of L 1527 and incorporate a central outflow region into both the two-layer and hill models. The resulting variation of T_{ex} with τ is shown schematically in Figure 4 (cf. Figure 1 of DeVries & Myers 2005).

3.3.1. Two-layer model with central outflow (2L-O model)

With the addition of a central outflow region to the two-layer model the line brightness temperature (equation 3) becomes,

$$\begin{aligned} \Delta T_B &= J(T_f)[1 - e^{-\tau_f}] + J(T_{out})[1 - e^{-\tau_{out}}]e^{-\tau_f} + J(T_r)[1 - e^{-\tau_r}]e^{-\tau_f - \tau_{out}} \\ &\quad -J(T_b)[1 - e^{-\tau_f - \tau_{out} - \tau_r}] \end{aligned} \quad (8)$$

where τ_{out} and T_{out} are the optical depth and excitation temperature of the outflow.

The only additional parameters needed in the 2L-O model are $\tau_{0,out}$ and σ_{out} the line center optical depth and the velocity dispersion of the outflow region. Both are used to calculate τ_{out} using,

$$\tau_{out} = \tau_{0,out} \exp\left[-(v - v_{LSR})^2 / 2\sigma_{out}^2\right]. \quad (9)$$

[1]The equation in DeVries & Myers (2005) is typeset incorrectly in the Astrophysical Journal. The correct version is found in the arXiv version (DeVries & Myers 2004)

In our model we set T_{out} equal to the average of T_r and T_f calculated using $\tau_{out,0}$ in equations 5a, 5b, 6a, and 6b as appropriate.

As a test of our version of the 2L-O model we were able to exactly match the model H_2CO ($J = 2 \rightarrow 1$) profile of L 1527 shown in Figure 3 of Myers et al. (1996) using the outflow and model parameters given in the figure caption.

3.3.2. Hill model with central outflow (Hill-O model)

The brightness temperature of the hill model with a central outflow is

$$\Delta T_B = (J_p - J_0)\left[\frac{1-e^{-\tau_f}}{\tau_f} - \frac{(1-e^{-\tau_r})e^{-\tau_f-\tau_{out}}}{\tau_r}\right] + (J_0 - J_b)(1-e^{-\tau_f-\tau_{out}-\tau_r}) \qquad (10)$$

where τ_{out} is the optical depth of outflow. Since we set the excitation temperature of the outflow equal to T_p (see Figure 4) the only additional parameters are $\tau_{0,out}$ and σ_{out}. As in the 2L-O model, τ_{out} is calculated using equation 9.

4. Results & Discussion

4.1. YSO Properties

We applied the 2L-O and the Hill-O models to our observed HCO^+ spectrum (see Figures 5 and 6 respectively). The best-fit parameters are given in Tables 1 and 2. Uncertainties were derived using a Monte Carlo method; an initial best fit of the model was obtained, then random noise at the same level as the observed line profile was added to the best fit and the resulting simulated line profile was then fit generating a new set of parameters. The standard deviation of spectral line parameters after 1000 repeats was combined with the mean fit uncertainties to produce the final error estimates.

As noted by Myers et al. (1996) the two-layer model tends to output profiles that have narrower peaks and flatter central troughs than observations, and both of these characteristics can be seen in the 2L-O best-fit model shown in Figure 5. In contrast the Hill-O model does a much better job in fitting the observed peak widths and the structure of the central absorption trough.

DeVries & Myers (2005) showed that Hill style models were able to obtain accurate estimates of infall velocities (rms error 0.01 km s^{-1}) from two-peak profiles in contrast with two-layer models, which tended to underestimate the infall velocity by factors of ~ 2.

Consistent with this finding, we see that the best-fit 2L-O V_{in} is a factor of 3.5 lower than the Hill-O value. While we adopt the numerical results of the Hill-O model for IRAS 01202+6133 we note that, regardless of the exact numeric values, both the 2L-O and Hill-O results are consistent with an object with a substantial envelope ($\tau_0 \sim 10$) undergoing slow infall ($V_{in} \ll \sigma$).

4.2. Formation Scenarios

There are two basic scenarios for the formation of IRAS 01202+6133, either its formation was triggered by the action of the expanding H II region or it formed spontaneously and its proximity to the H II region is coincidental.

To gauge the likelihood of the first scenario we can first look at the various time scales associated with the YSO-H II region system. The canonical duration of the Class I stage of YSO evolution is of order 10^5 years (Ward-Thompson 2002). The fact that IRAS 01202+6133 still has a substantial envelope and exhibits slow infall suggests that it is still a fairly young Class I YSO. The presence of outflow motions does not constrain the age as they are known to be associated with even the very earliest stages of YSO evolution (André et al. 1993). Assuming that any Class 0 stage would be very rapid ($\sim 10^4$ years), we conclude that the age of the YSO is $\tau_{YSO} \leq 10^5$ years. KR 120 is a fairly young H II region, Joncas et al. (1992) estimate an age $\tau_{HII} \approx 1 - 2 \times 10^5$ years based on kinematic and photodissociation region models for the region. So it appears that a necessary condition for triggered formation, that $\tau_{YSO} < \tau_{HII}$, is just satisfied in this case.

As mentioned in § 1, triggered star formation around H II regions can arise from the overpressurization of existing cores or through the collapse of a swept up layers of material. To investigate the latter "collect and collapse" scenario we use the equation from Whitworth et al. (1994) giving the timescale at which fragmenation and collapse will occur in a swept-up shell around an expanding H II region:

$$t_{fragment} \approx 1.56 \text{ Myr} \quad \left[\frac{a_s}{0.2 \text{ km s}^{-1}}\right]^{7/11} \left[\frac{Q_0}{10^{49} \text{ ph s}^{-1}}\right]^{-1/11} \left[\frac{n_0}{1000 \text{ cm}^{-3}}\right]^{-5/11}, \qquad (11)$$

where a_s is sound speed of the molecular cloud, Q_0 is the H I ionizing flux, and n_0 is the density of the molecular cloud. The exciting star of KR 120 is B0 V (Arvidsson & Kerton 2011) corresponding to Q_0=$10^{47.4}$ ph s^{-1} using the Crowther (2005) calibration. For n_0 we use the value $n_0 = 1000$ cm^{-3} from Joncas et al. (1992). A fragmetation collapse timescale is approximately between 2 Myr with sound speed $a_s = 0.2$ km s^{-1} (very cold molecular clouds) and up to a 6 Myr upper limit with with $a_s = 1$ km s^{-1} (warm molecular/neutral

clouds). Since this fragmentation timescale is 10 times longer than τ_{HII} we can eliminate the "collect and collapse" triggered star formation scenario.

The morphology of the molecular cloud surrounding KR 120 (see Figure 7) is consistent with the alternative scenario of triggered collapse of a pre-exisiting molecular core. The highest column density gas (e.g., $T_B > 50$ K km s^{-1}), where one would expect to find molecular cloud cores, lies in a ridge to one side of the H II region. In this picture a shock front being driven into this gas by the expanding H II region has overrun and compressed an pre-existing core initiating the star formation process (Bertoldi 1989; Thompson et al. 2004).

We cannot rule out a spontaneous star formation scenario; it is possible that the YSO happened to form at the correct distance from the exciting star of KR 120 that it now lies on the edge of the expanding H II region. On balance though, we prefer the triggered scenario as it naturally explains the close spatial association of the H II region and the very young Class I YSO.

5. Conclusions

1. Our analysis of the HCO^+ ($J = 3 \rightarrow 2$; 267.6 GHz) and $H^{13}CO^+$ ($J = 3 \rightarrow 2$; 260.3 GHz) spectra of the submm/IR source IRAS 01202+6133 shows that the blue-asymmetric HCO^+ line profile is almost certainly due to infall motions.

2. We have modified the analytic radiative transfer models of Myers et al. (1996) and DeVries & Myers (2005) to allow for fitting of submm/mm line profiles that have both self-absorption features and optically thin wings. We applied these models to our HCO+ submm spectrum of IRAS 01202+6133 and conclude that it is a young Class I YSO with a substantial envelope undergoing slow infall.

3. Based on its young evolutionary state ($\tau_{YSO} < \tau_{HII}$), and its proximity to the H II region KR 120 (Sh 2-187), we think that the formation of IRAS 01202+6133 was triggered by the expansion of the H II region. However, due to young age of the H II region a "Collect and Collapse" scenario is ruled out.

We would like to thank Dr. Lewis B. G. Knee for his assistance with the processing of the JCMT data.

Facilities JCMT

REFERENCES

André, P., Ward-Thompson, D., & Barsony, M. 1993, ApJ, 406, 122

Arvidsson, K. & Kerton, C. R. 2011, AJ, 141, 153

Bertoldi, F. ApJ, 346, 735

Crowther, P.A. 2005, in IAU Symp. 227, Massive Star Birth: A Crossroads of Astrophysics, ed. R. Cesaroni, M. Felli, E. Churchwell, & M. Walmsley (Cambridge: Cambridge Univ. Press), 389

Deharveng, L., Lefloch, B., Zavagno, A., Caplan, J., Whitworth, A.P., Nadeau, D., & Martin, S. 2003, A&A, 408, 25

DeVries, C.H.& Myers, P.C. 2004, arXiv:astro-ph/0410748

DeVries, C.H. & Myers, P.C. 2005, ApJ, 620, 800

Elmegreen, B.G. 1998, in ASP Conf. Ser. 148, Origins, ed. C.E. Woodward, J.M. Shull, & H.A. Thronson (San Francisco, CA: ASP), 150

Elmegreen, B.G. & Lada, C.J. 1977, ApJ, 214,725

Heyer, M.H., Brunt, C., Snell, R.L., Howe, J.E., Schloerb, F.P., & Carpenter, J.M. 1998, ApJS, 115, 241

Hosokawa, T. & Inutsuka, S. 2006 ApJ, 646, 240

Joncas, G., Durand, D., & Roger, R.S. 1992, ApJ, 387, 591

Kalas, E. & Reich, W. 1980, A&AS, 42, 227

Myers, P.C., Mardones, D., Tafalla, M., Williams, J.P., & Willner, D.J. 1996, ApJ, 465, 133

Price, S.D., Egan, M.P., Carey, S.J., Mizuno, D.R., & Kuchar, T.A. 2001, AJ, 121, 2819

Sharpless, S. 1959, ApJS, 4, 257

Sun, Y., & Gao, Y. 2009, MNRAS, 392, 170

Taylor, A.R. et al. 2003, AJ, 125, 3145

Thompson, M.A., White, G.J., Morgan, L.K., Miao, J., Fridlund, C.V.M, Huldtgren-White, M. 2004, A&A, 414, 1017

Ward-Thompson, D. 2002, Science, 295, 76

Whitworth, A.P., Bhattal, A.S., Chapman, S.J., Disney, M.J., & Turner, J.A MNRAS, 268, 291

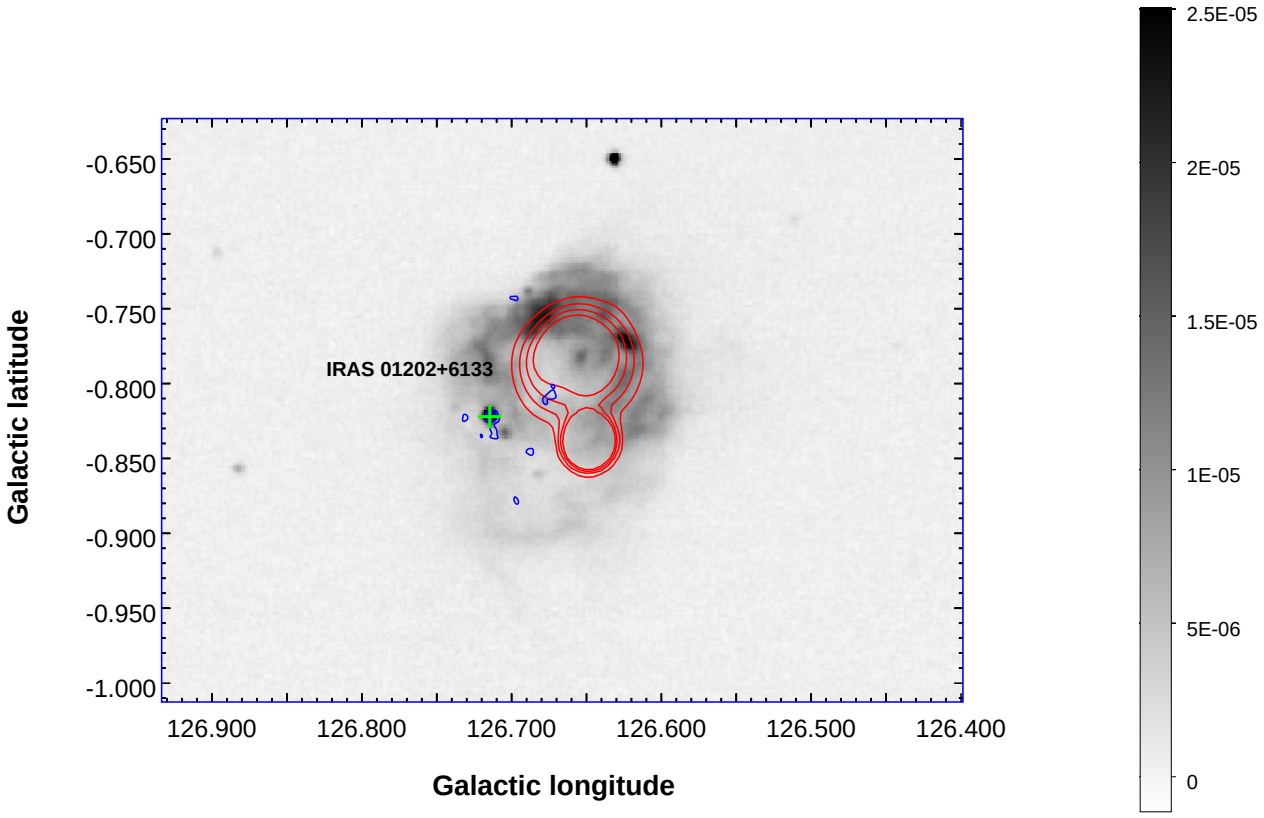

Fig. 1.— The H II Region KR 120 (Sh2-187). This *Midcourse Space Experiment* (*MSX*; Price et al. 2001) 8.3 μm image traces emission from the photodissociation region within the molecular cloud surrounding KR 120. The red contours correspond to Canadian Galactic Plane Survey (CGPS; Taylor et al. 2003) 1420 MHz continuum emission at T_B = 8, 10, 12 and 14 K. The elongated radio source seen at the bottom of the main H II region is extragalactic. The blue contours represent SCUBA 850 μm continuum with levels of 1.2×10^{-3}, 2×10^{-3}, 3×10^{-3}, 6×10^{-3} Jy beam^{-1}. Note the location of the Class I YSO IRAS 01202+6133 on the periphery of the H II region.

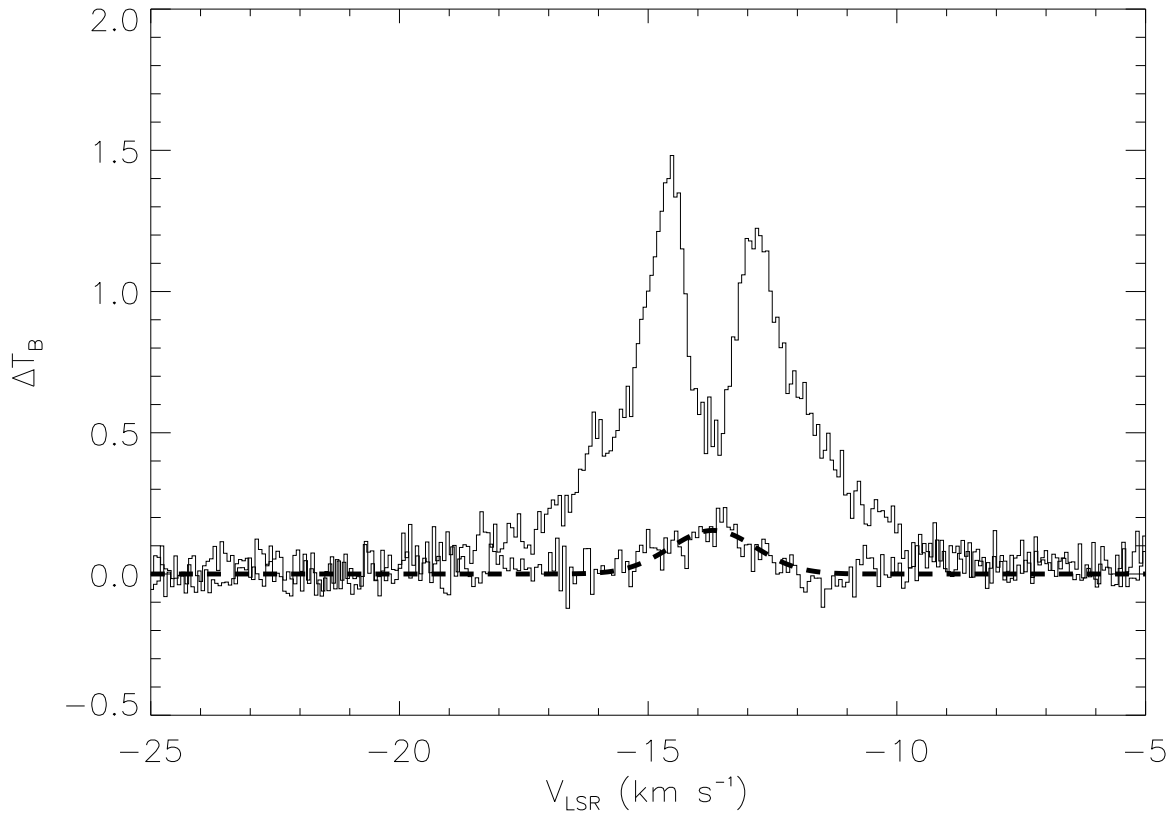

Fig. 2.— HCO^+ spectra of IRAS 01202+6133. The HCO^+ ($J = 3 \rightarrow 2$; 267.6 GHz) line has a classic blue asymmetric line profile. The optically thin $H^{13}CO^+$ ($J = 3 \rightarrow 2$; 260.3 GHz) line (with Gaussian fit shown) peaks at the minimum between two peaks of HCO^+ line confirming that blue asymmetric line shape comes from the infall motion.

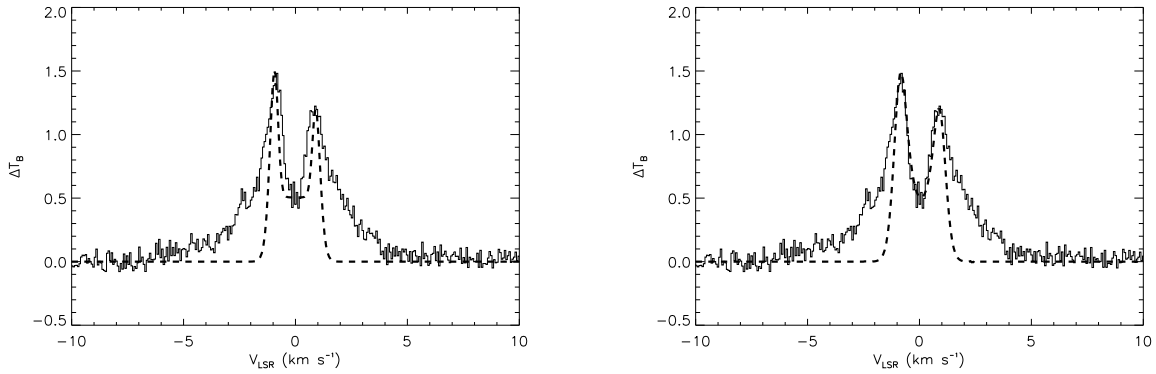

Fig. 3.— Basic model results. The figure shows how the basic Two-Layer model (left) and Hill model (right) are unable to fit the extended wings seen in the HCO^+ spectrum. In these plots the systematic velocity of the cloud ($V_{LSR} = -13.7$ km s^{-1}) has been removed.

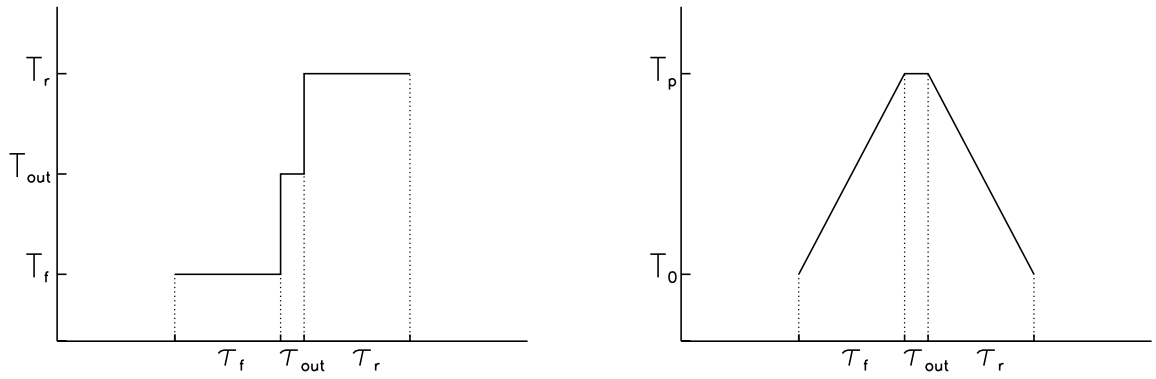

Fig. 4.— Modified radiative transfer models. In order to fit the extended wings seen in the HCO^+ spectrum we added a central low optical depth "outflow" region to the exisiting two-layer and hill models. The diagrams schematically show the run of temperature with optical depth in the 2L-O model (left) and Hill-O model (right).

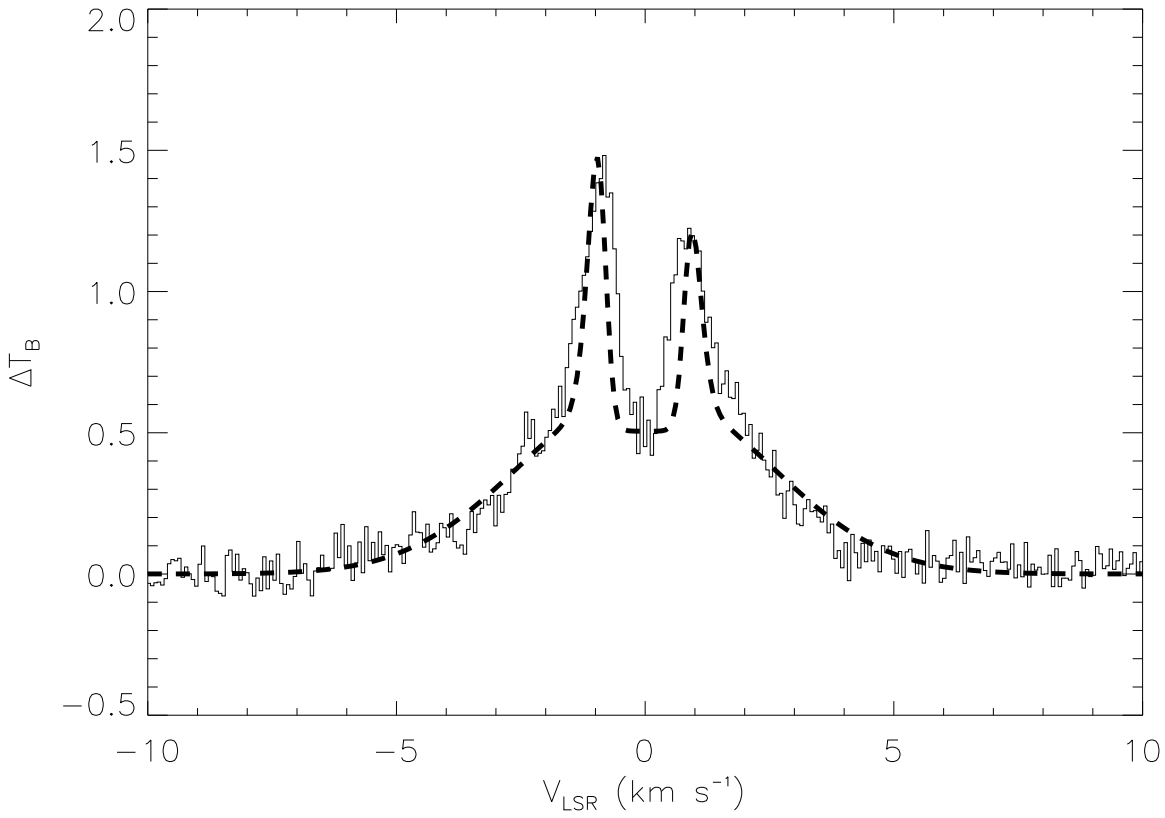

Fig. 5.— Best fit 2L-O model. The model is able to fit the extended wings of the HCO^+ line, but as expected for a two-layer model has some trouble matching the line widths and the trough structure. The best fit parameters are given in Table 1 and the systematic velocity of the YSO has been removed from this plot.

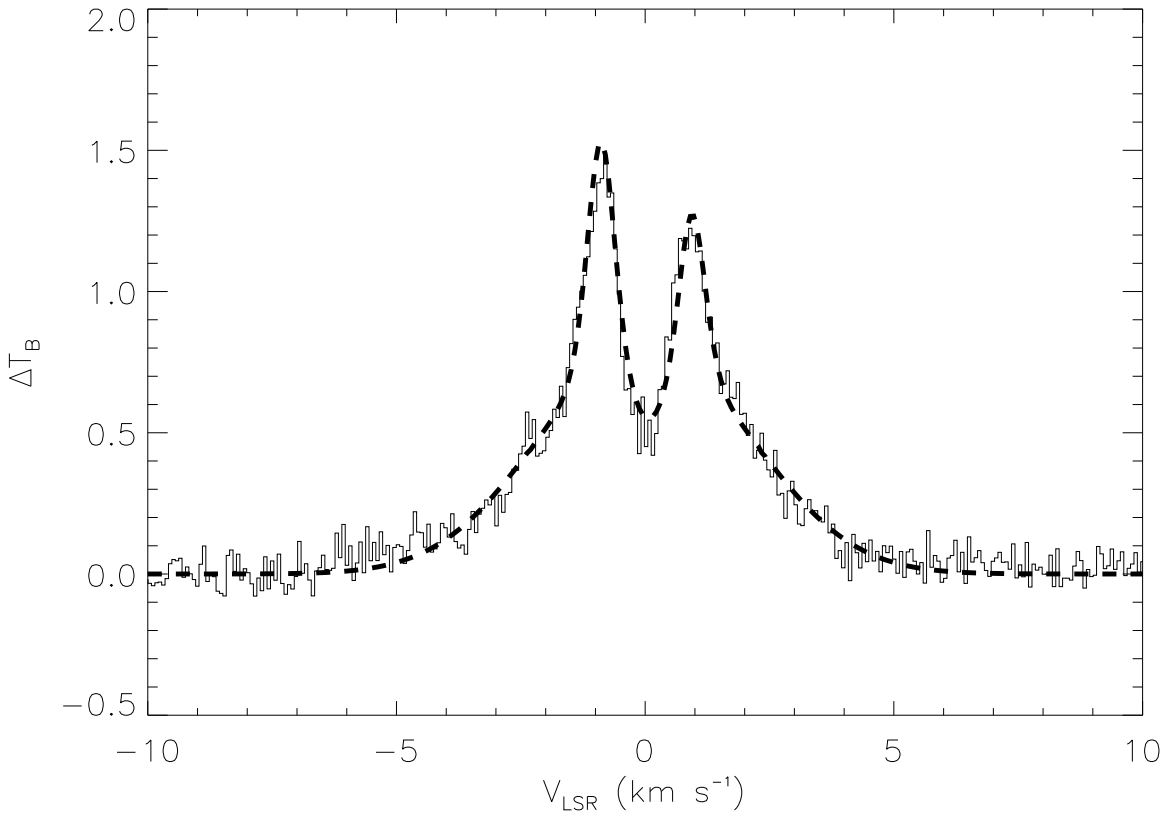

Fig. 6.— Best fit Hill-O model. The model is able to fit the extended wings of the HCO^+ line and has a better fit to the central portions of the line profile compared to the 2L-O model. The best fit parameters are given in Table 2 and the systematic velocity of the YSO has been removed from this plot.

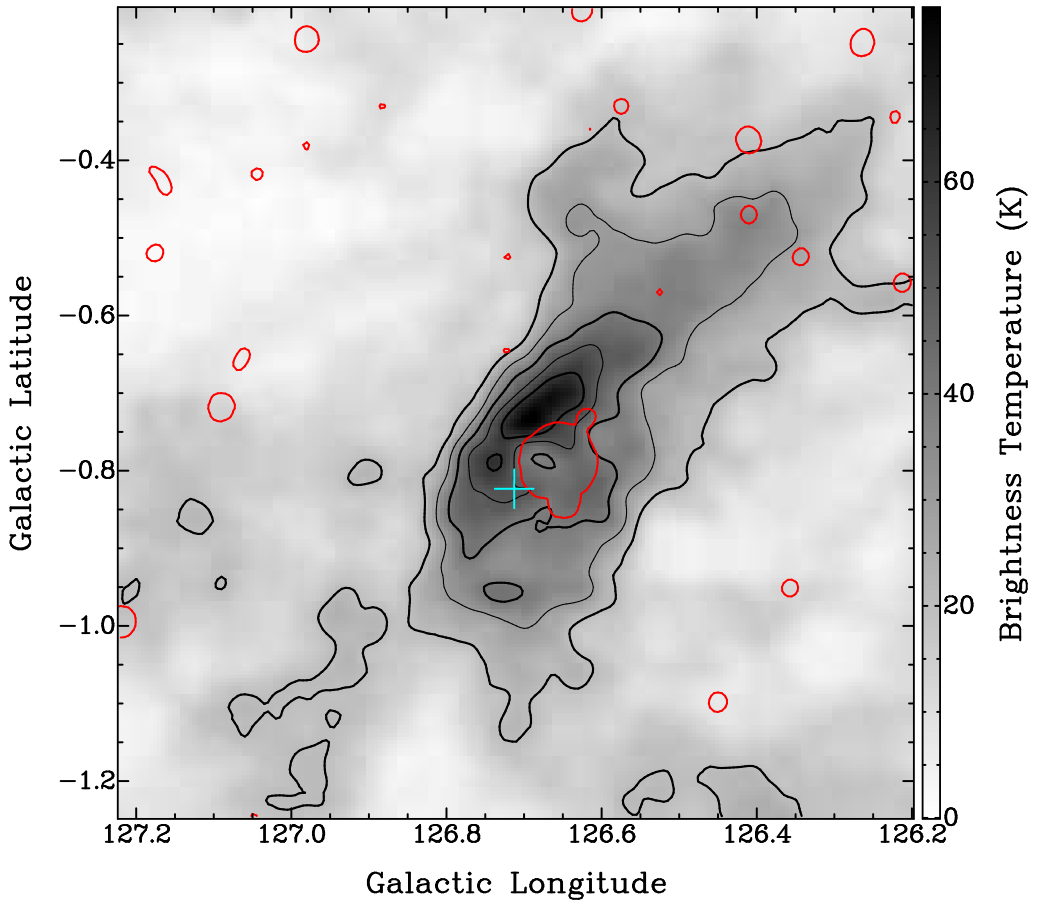

Fig. 7.— The molecular cloud of KR 120. The image is ^{12}CO ($J = 1 \rightarrow 0$) emission from the Outer Galaxy Survey (Heyer et al. 1998) integrated between $-20.4 < V_{LSR} < -5.6$ km s^{-1} (contours at 20, 30, 40, 50, and 60 K km s^{-1}). The position of KR 120 is shown by the red contour at $T_{1420} = 8$ K, and the position of IRAS 01202+6133 is indicated by the cross.

Table 1. Best Fit Free Parameters of 2L-O model

τ_0	V_{LSR} (km s^{-1})	T_K (K)	V_{in}(km s^{-1})	σ_{NT}(km s^{-1})	τ_{out}	σ_{out}(km s^{-1})
11 ± 0.2	-13.74 ± 0.01	9.5 ± 0.15	0.02 ± 0.003	0.4 ± 0.01	0.35 ± 0.01	2.3 ± 0.03

Note. — Background temperature is set at $T_b = 2.725$ K. Uncertainties are obtained by a Monte Carlo method with 1000 repetitions.

Table 2. Best Fit Free Parameters of Hill-O model

τ_c	V_{LSR} (km s^{-1})	V_{in} (km s^{-1})	σ(km s^{-1})	T_p (K)	T_0 (K)	τ_{out}	σ_{out}(km s^{-1})
6.5 ± 0.1	-13.74 ± 0.01	0.07 ± 0.012	0.47 ± 0.02	7.7 ± 0.13	3.2 ± 0.22	0.32 ± 0.03	2 ± 0.06

Note. — Background temperature is set at $T_b = 2.725$ K. Uncertainties are obtained by a Monte Carlo method with 1000 repetitions.